



U.S. Department
of Transportation

**National Highway
Traffic Safety
Administration**



DOT HS 812 758

July 2019

Determination of Optimal RibEye LED Locations in The WorldSID 50th Percentile Male Dummy

DISCLAIMER

This publication is distributed by the U.S. Department of Transportation, National Highway Traffic Safety Administration, in the interest of information exchange. The opinions, findings and conclusions expressed in this publication are those of the authors and not necessarily those of the Department of Transportation or the National Highway Traffic Safety Administration. The United States Government assumes no liability for its contents or use thereof. If trade or manufacturers' names are mentioned, it is only because they are considered essential to the object of the publication and should not be construed as an endorsement. The United States Government does not endorse products or manufacturers.

Suggested APA Format Citation:

Rhule, H., Millis, W., Mallory, A., & Stricklin, J. (2019, July). *Determination of optimal RibEye LED locations in the WorldSID 50th percentile male dummy* (Report No. DOT HS 812 758). Washington, DC: National Highway Traffic Safety Administration.

1. Report No. DOT HS 812 758		2. Government Accession No.		3. Recipient's Catalog No.	
4. Title and Subtitle Determination of Optimal RibEye LED Locations in the WorldSID 50th Percentile Male Dummy				5. Report Date July 2019	
				6. Performing Organization Code	
7. Authors Heather Rhule, William Millis, NHTSA's Vehicle Research and Test Center; Ann Mallory, Jim Stricklin, Transportation Research Center Inc.				8. Performing Organization Report No.	
9. Performing Organization Name and Address Vehicle Research and Test Center, East Liberty, Ohio; Transportation Research Center Inc., East Liberty, Ohio				10. Work Unit No. (TRAVIS)	
				11. Contract or Grant No.	
12. Sponsoring Agency Name and Address National Highway Traffic Safety Administration 1200 New Jersey Avenue SE Washington, DC 20590				13. Type of Report and Period Covered Final Report	
				14. Sponsoring Agency Code	
15. Supplementary Notes					
16. Abstract This report documents the methods and results of testing and analysis to determine optimal locations for RibEye LEDs to measure chest deflection in the WorldSID 50th Percentile Male Dummy. This study determined that the optimal locations for the front and rear chest deflection measurements, along with the lateral-most location, which is currently measured, occur at a linear distance of 35 mm in the x direction with respect to the lateral-most location. Using these optimal measurement locations, estimated deflections resulted in a worst-case error of 9 mm and a mean error of 1.1-1.4 mm. In comparison, measuring deflection in the current tests at only a single location (lateral-most location), would have resulted in a maximum error of 23 mm, and an average error of 4.7 mm. This project supports NHTSA's mission to reduce the number of deaths and injuries by studying how best to position chest deflection sensors to measure maximum deflection, which is used to estimate injury risk in crash tests.					
17. Key Words RibEye, virtual RibEye, WorldSID-50M, male test dummy, 50th percentile, IR-TRACC				18. Distribution Statement Document is available to the public from the National Technical Information Service, www.ntis.gov.	
19. Security Classif. (of this report) Unclassified		20. Security Classif. (of this page) Unclassified		21. No. of Pages 36	22. Price

Form DOT F 1700.7 (8-72)

Reproduction of completed page authorized

Table of Contents

1	INTRODUCTION	1
2	METHODS	7
	2.1 Dynamic Rib Testing.....	7
	2.2 Predicted Deflection at Virtual RibEye LED Locations.....	11
	2.3 Methods for Optimization of RibEye LED Locations.....	16
3	RESULTS	17
	3.1 Dynamic Rib Testing.....	17
	3.2 Combinations of RibEye LED Locations	19
	3.3 Deflection Comparisons Among Overall Max, Max of Trio of Virtual LED Positions, and IR-TRACC	22
4	DISCUSSION	27
	4.1 Deflection Comparisons Among Overall Max, Max of Trio of Virtual LED Positions, and IR-TRACC	27
5	CONCLUSIONS	29

List of Figures

Figure 1. WorldSID-50M IR-TRACC deflection measurement instrumentation. View of dummy is from overhead at an oblique angle.....	1
Figure 2. ES-2re (left; head and neck removed) and SID-IIs (right) measure deflection with linear potentiometers. View of each dummy is from overhead.	2
Figure 3. RibEye sensors (left) and LEDs (right) installed in the WorldSID-50M. Note that for a group of three sensors, the sensors for the top and bottom ribs are mounted at an angle, and the sensor for the middle rib is mounted flat. View is from pelvis upward. Photo copyright by Boxboro Systems	3
Figure 4. Close-up view of LEDs mounted to ribs. Circles denote angled mounting blocks on the top and bottom ribs (yellow and red), and no mounting block on the middle rib (white). Photo copyright by Boxboro Systems	3
Figure 5. Schematic showing left side cross-section view of thorax with RibEye sensors. Upper set of sensors shown in pink; lower set of sensors shown in blue. RibEye origins denoted by red dots; x and z axes directions defined by the orientation of the origin sensor for each set of sensors. Dimensions indicate location of center of top and bottom sensors from the origin for the upper and lower sets of three sensors.	5
Figure 6. Schematic showing inner rib prior to impact and deformed at some time t , LEDs (red), origin at the rib of interest (green), and lengths between the front LED and the origin at time zero (l_0) and at time t , ($l(t)$). The change in length is $l_0 - l(t)$	6
Figure 7. Test setup for 30° posterior-to-lateral (left) and 20° anterior-to-lateral (right) impacts.....	8
Figure 8. Pre-impact image for thorax rib 3 impacts. (Note that multiple RibEye LEDs are mounted on the inner surface of the rib. This data is discussed in the previously referenced report that evaluates the usefulness and accuracy of RibEye measurements.).....	10
Figure 9. Initial position of Virtual RibEye LED corresponding to target P10 on thoracic rib 3	12
Figure 10. Close-up of initial position of Virtual RibEye LED corresponding to target P10 on thoracic rib 3	13
Figure 11. Rib angle $\beta(t)$ of Virtual RibEye location corresponding to target P2 on thoracic rib 3 in dynamic test 30 degrees posterior-to-lateral	14
Figure 12. Calculation of distance dt from VR LED to origin at time t	15
Figure 13. Pre-impact and maximum deflection images for thorax rib 3 lateral (a and b), 30° posterior (c and d), and 30° anterior (e and f) impacts. (Note that multiple RibEye LEDs are mounted on the inner surface of the rib. This data is discussed in <i>Evaluation of RibEye Installed in the WorldSID 50th Percentile Male Dummy</i> , a report still being prepared by NHTSA’s Vehicle Research and Test Center.)	18
Figure 14. Image of thorax rib 1 showing final locations selected for the three LEDs, anterior and posterior targets of the five best combinations, and rib damping material taper	21
Figure 15. Schematic of a rib showing the final locations for the three LEDs	22
Figure 16. Deflection time histories for overall max deflection, A6/0/P6 combination, and IR-TRACC location for +30° and +20° dynamic impact tests for thorax ribs 1, 2, and 3	23
Figure 17. Deflection time histories for overall max deflection, A6/0/P6 combination, and IR-TRACC location for -30° and -20° dynamic impact tests for thorax ribs 1, 2, and 3	24

Figure 18. Deflection time histories for overall max deflection, A6/0/P6 combination, and IR-TRACC location for +10°, -10°, and 0° dynamic impact tests for thorax ribs 1, 2, and 3.....	25
Figure 19. Max deflection for each virtual LED position for thorax rib 1 (a), thorax rib 2 (b), and thorax rib 3 (c) in all dynamic rib impacts.....	26
Figure 20. Differences in max deflection reported between overall max deflection and A6/0/P6 and IR-TRACC locations.....	28

1 Introduction

The WorldSID 50th percentile male dummy (WorldSID-50M) comes instrumented at each rib (six ribs total) with an InfraRed -Telescoping Rod for Assessment of Chest Compression (IR-TRACC). The IR-TRACC is mounted between the spine box and the lateral-most part of the rib and measures the change in length between these two points (Figure 1). There is also a rotary potentiometer that can be mounted along with the IR-TRACC, which will track the rotation of the rib at the IR-TRACC location about the z axis. Used together, the 2D IR-TRACC can be used to calculate the x and y components of the change in length between the lateral-most portion of the rib and the spine box.

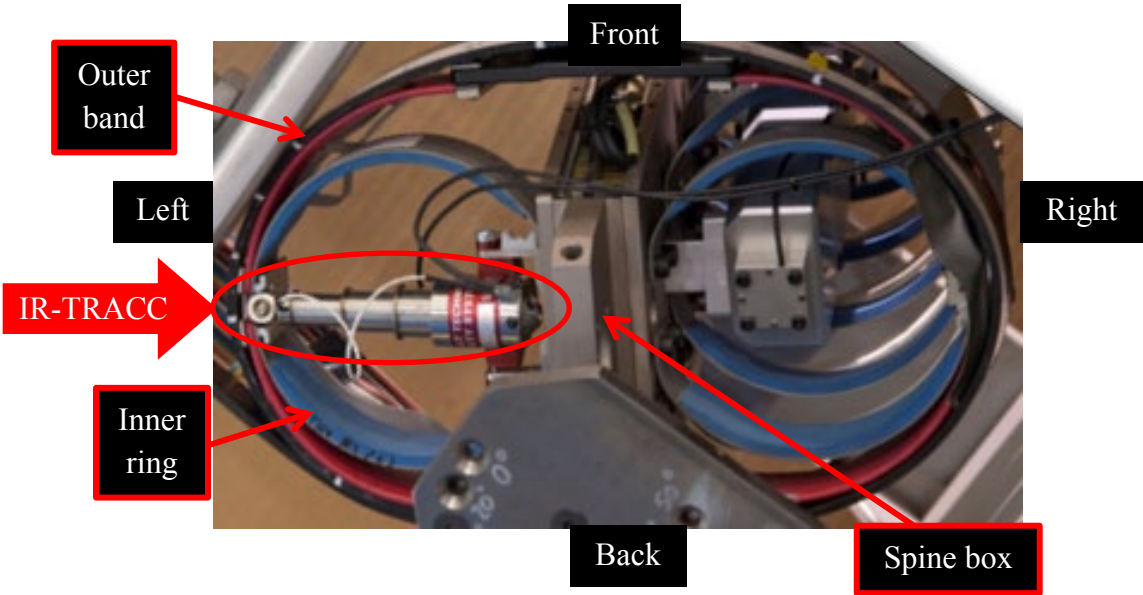


Figure 1. WorldSID-50M IR-TRACC deflection measurement instrumentation. View of dummy is from overhead at an oblique angle.

The location of maximum deflection of a rib will vary depending on the impact location and direction. Thus, if there is loading to the rib at some point other than its lateral-most point where the IR-TRACC is mounted, the IR-TRACC may not capture the full amount of deflection that occurs to the rib. The WorldSID-50M is not the only side impact dummy with this measurement issue. The ES-2re and SID-IIs also measure deflection at a single point on the rib, with a linear potentiometer (Figure 2). Therefore, measuring deflection at multiple locations on the rib will increase the likelihood that the maximum measured deflection will be close to the rib’s actual maximum deflection, which is important because maximum deflection is the best predictor of thoracic injury.

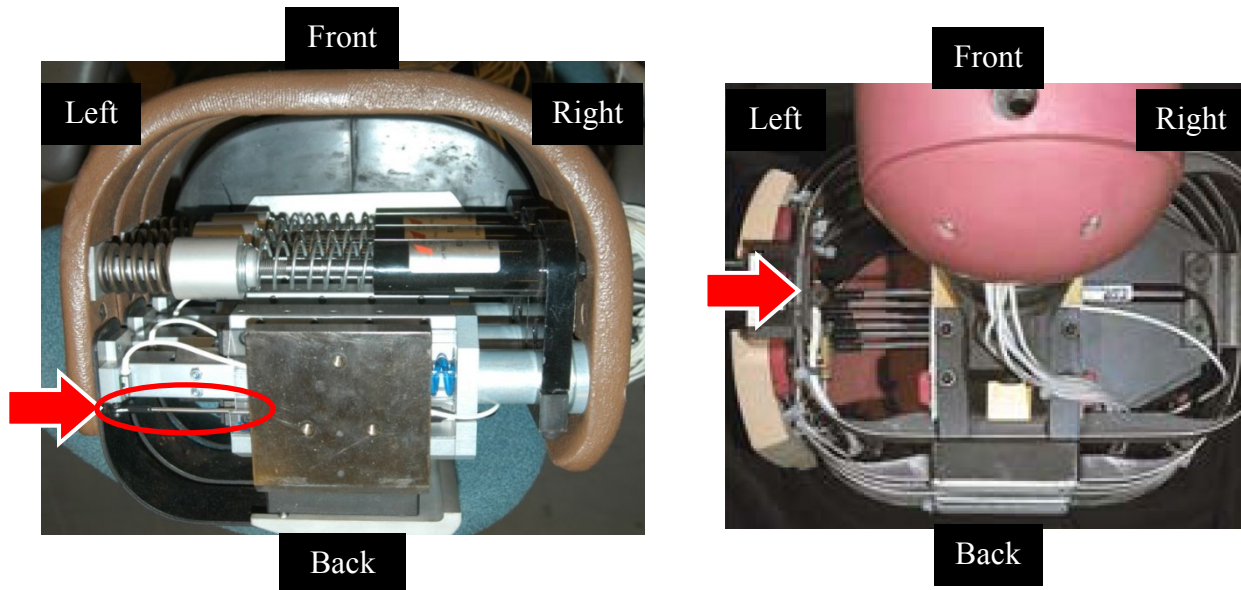


Figure 2. ES-2re (left; head and neck removed) and SID-IIs (right) measure deflection with linear potentiometers. View of each dummy is from overhead.

A relatively new instrument called RibEye Multi-Point Deflection Measurement System is available for use in the WorldSID-50M. When configured for the WorldSID-50M, the RibEye consists of two groups of three sensors (receivers) mounted on the impact side of the spine box, one at each rib level, and three light emitting diodes (LEDs) per rib, mounted on the inner surface of the inner rib on the impact side (Figure 3). The RibEye measures x, y, and z positions for each LED at 10,000 samples per second. The top set of sensors uses red optical filters and monitors the red LEDs mounted on the top three ribs (shoulder, thorax rib 1, and thorax rib 2). The bottom set of sensors uses blue optical filters and monitors the blue LEDs mounted on the bottom three ribs (thorax rib 3, abdomen ribs 1 and 2). Within each group of three sensors, position data from each sensor is reported with respect to a coordinate system that has its origin in the middle sensor of each set. Within each group of three sensors, the LEDs are installed using angled mounting blocks on the top and bottom ribs, and no mounting block on the middle rib (Figure 4). Note that the sensors (Figure 3) are also angled on the top and bottom ribs and flat on the middle rib. The LEDs and sensors are mounted this way so that the LED light is better aimed toward the sensors. The RibEye also includes its own data acquisition system and controller, which are installed on the non-impact side of the spine box. Each sensor has a finite field of view, within which it can sense the position of the LEDs. If an LED moves outside the field of view of the sensor, its position can no longer be sensed, and an error code will be produced by the RibEye software.

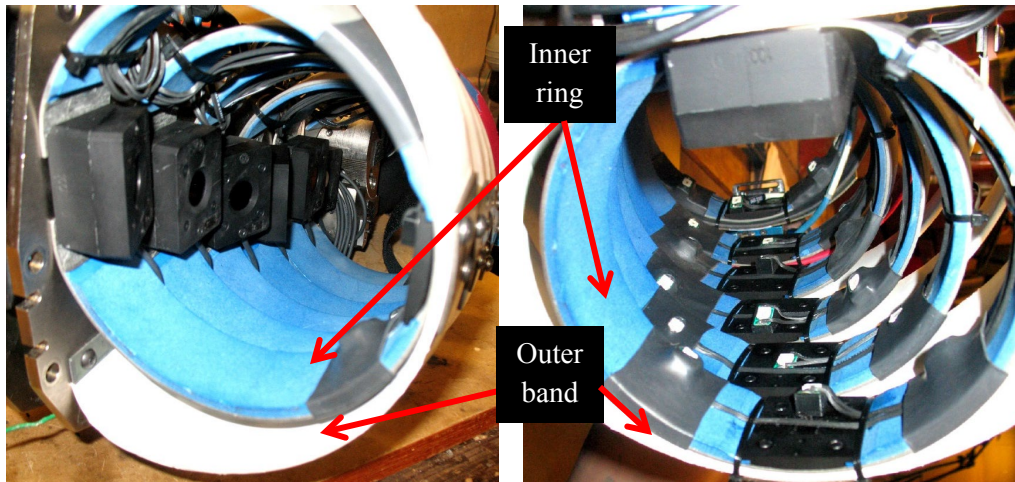


Figure 3. RibEye sensors (left) and LEDs (right) installed in the WorldSID-50M. Note that for a group of three sensors, the sensors for the top and bottom ribs are mounted at an angle, and the sensor for the middle rib is mounted flat. View is from pelvis upward. Photo copyright by Boxboro Systems

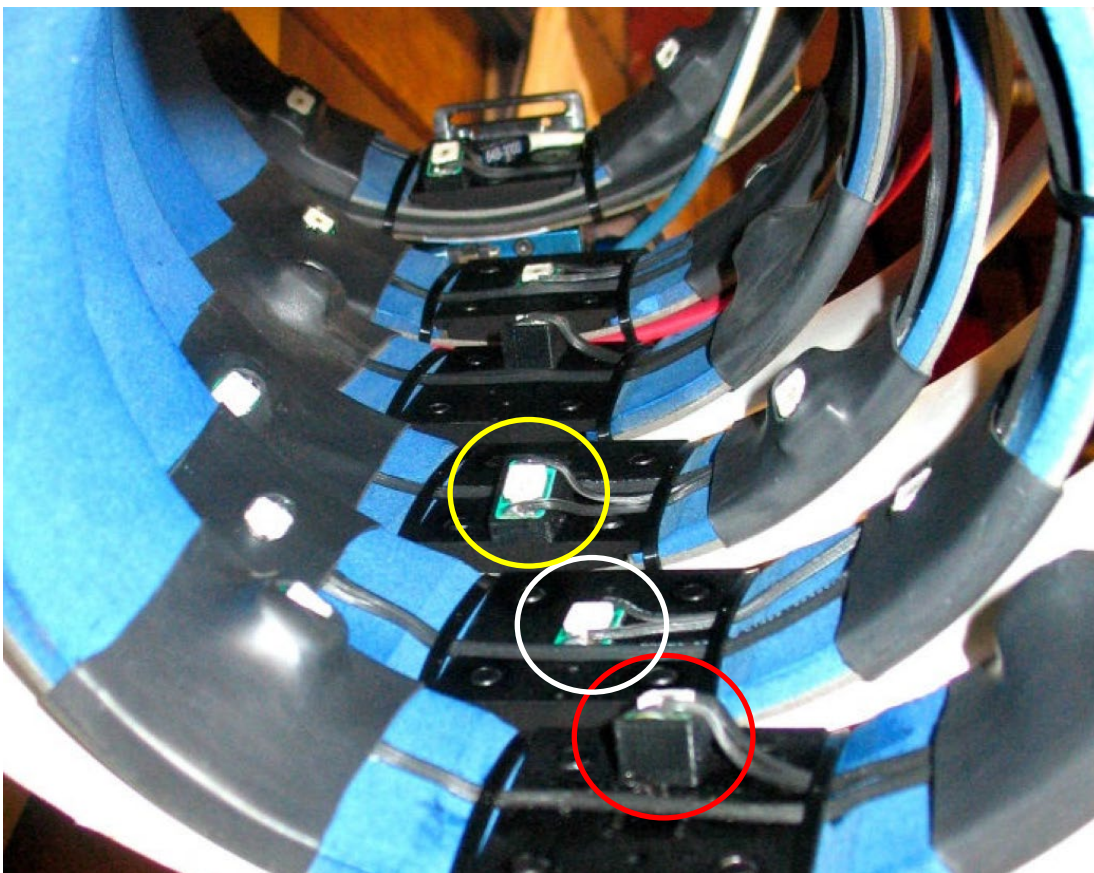


Figure 4. Close-up view of LEDs mounted to ribs. Circles denote angled mounting blocks on the top and bottom ribs (yellow and red), and no mounting block on the middle rib (white). Photo copyright by Boxboro Systems

In order to assess injury, deflection toward the spine is calculated from the x and y position data from the RibEye as the xy change in length (or deflection) of the LED from the RibEye origin. However, since the RibEye origin is located at the middle sensor for each group of three sensors, in order to measure the xy length change for each LED, the origin is first translated to the same relative location for the rib of interest (i.e., for the shoulder rib, the middle sensor origin at thorax rib 1 is translated to the top sensor at the shoulder rib). Although the WorldSID-50M ribs are offset in the x (anterior-posterior) and z (superior-inferior) directions, the rib deflections are measured in the xy plane, so the RibEye origin need only be translated in the x direction so that the rib deflections will be measured relative to the (x,y) position of the sensor of the rib of interest (Figure 5). For example, if we are interested in the xy deflection of thorax rib 2, the RibEye origin would need to be translated in the x direction from its location at the middle sensor of thorax rib 1. Then, the change in length is calculated as shown in Equations 1-3 and Figure 6 for any time, t . This measurement is similar to the change in length of the IR-TRACC telescoping tube.

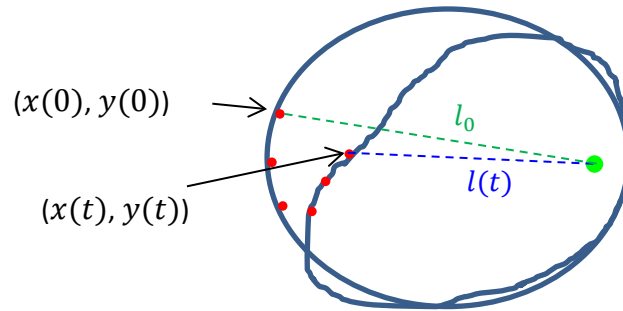


Figure 6. Schematic showing inner rib prior to impact and deformed at some time t , LEDs (red), origin at the rib of interest (green), and lengths between the front LED and the origin at time zero (l_0) and at time t , ($l(t)$). The change in length is $l_0 - l(t)$.

The WorldSID-50M ribs include a very compliant outer band and a smaller-diameter, stiffer steel inner ring, as shown in Figures 1 and 3. The inner ring and outer band are attached at the lateral-most point (where the IR-TRACC is typically mounted). During an impact to the anterior-lateral or posterior-lateral aspect of the rib, the outer band can easily flatten and come into contact with the inner ring. The RibEye does not measure the deflection of the outer band as it flattens. Since only the deflection of the inner ring is measured, there is not a one-to-one correspondence with human chest deflections (as measured by chest bands) and WorldSID-50M RibEye measurements at the anterior-lateral and posterior-lateral aspects. The WorldSID-50M RibEye deflections will always be less than those measured by chest bands in PMHS. However, as long as the dummy measurement correlates well with injury risk, this discrepancy should be inconsequential. Injury risk curves developed with WorldSID-50M RibEye data are reported.¹

Because chest deflection is used for assessing injury, it is critical that the maximum measured chest deflection is as close as possible to the actual maximum chest deflection that occurred. The ideal locations for measuring deflection are those that minimize the error between the *actual* maximum deflection of a rib and the *measured* maximum deflection across the spectrum of possible impact conditions. In order to select the ideal locations for the three RibEye LEDs on each rib, the deformation of ribs during a series of dynamic tests was analyzed. In that testing, the deformation of fiducial targets along each individual rib was tracked using high-speed video. However, the locations of the targets on the rib (top surface of the rib) are not the same as the locations where the LEDs would be placed (inner surface of the rib, with or without an angled mounting block). Thus, the deflection that would be measured at virtual RibEye (VR) LED locations near each fiducial target was calculated, relative to the translated RibEye origin at each rib level, using the tracked deformation at each target. In that way, the deflection that would be measured at VR LEDs was predicted along each rib over a range of different impacts. At any

¹ *WorldSID 50th Percentile Male Side Impact Dummy Injury Risk Functions*, a report still being prepared by NHTSA's Vehicle Research and Test Center

given time, the maximum predicted deflection among the VR positions was assumed to be the true maximum deflection of the rib. Using the predicted deflection at each VR LED location, as well as the maximum predicted deflection among all VR positions (deemed true maximum deflection) on the rib throughout the time-history of the dynamic tests, the optimal combination of three RibEye LED locations was determined.

2 METHODS

2.1 Dynamic Rib Testing

In order to determine the optimal combination of three LED locations, dynamic rib testing was performed with high-speed video analysis. The full WorldSID-50M dummy was used for the tests, with the exception of the head, neck, shoulder, arm, and any ribs above (and sometimes below) the rib being impacted, so that the top surface of the rib being impacted could be viewed by the camera. The sternum was installed for the rib being impacted. Single ribs were impacted using a hydraulic linear impactor with a 152 mm diameter probe face with a mass of 23 kg. The speed of impact was adjusted between 2.0 and 4.3 m/s such that a large amount of deflection was observed, but not so much as to damage the rib. Each thoracic rib was impacted at several angles to cover the range of potential impact angles that might occur in a crash test. Table 1 shows the test matrix. Because the shoulder and abdomen rib dynamic impact responses may be different than those of the thoracic ribs, it would have been ideal to test all of the ribs, and use data from all of the ribs to determine the optimal combination of three LED locations for all ribs. However, due to logistical complications with conducting these tests on the shoulder (i.e., interference between the impactor and arm during oblique impacts) and abdomen (i.e., interference between the pelvis and impactor, as well as interference between abdomen rib 2 and the pelvis) ribs, only the three thoracic ribs were tested.

Table 1. Dynamic Rib Impact Test Matrix

Thorax rib 1	Thorax rib 2	Thorax rib 3
30° posterior-to-lateral	30° posterior-to-lateral	30° posterior-to-lateral
20° posterior-to-lateral	20° posterior-to-lateral	20° posterior-to-lateral
10° posterior-to-lateral	10° posterior-to-lateral	10° posterior-to-lateral
0° lateral	0° lateral	0° lateral
10° anterior-to-lateral	10° anterior-to-lateral	10° anterior-to-lateral
20° anterior-to-lateral	20° anterior-to-lateral	20° anterior-to-lateral
30° anterior-to-lateral	30° anterior-to-lateral	30° anterior-to-lateral
Impact velocities were adjusted per test between 2.0 and 4.3 m/s		

For lateral impacts, the dummy was seated on the qualification bench. For posterior-to-lateral impacts, the dummy was seated directly on the test table, without the qualification bench. For anterior-to-lateral impacts, the dummy was seated on the qualification bench with car seat foam

mounted in a frame behind the dummy's torso. These test conditions were selected in order to load the ribs at various impact angles, while capturing the rib motion with video and attempting to keep the conditions somewhat realistic relative to what a dummy would experience in a crash test (MDB and pole crash tests performed with a chest band installed on thorax rib 1 of the WorldSID-50M dummy in the driver seat achieved maximum deflection at angles ranging between -22° and $+44^{\circ}$ from lateral).² For the posterior and anterior impacts, the dummy was rotated about the spine 10, 20 or 30 degrees. To achieve the appropriate impact angle, a protractor was placed on the monitor showing the view from the overhead camera and the center of the dummy's spine was aligned to the desired angle. After rotating the dummy, the dummy was shifted forward or rearward such that the center of the probe face was aligned with the outermost portion of the rib. A 152 mm x 40 mm x 12.7 mm piece of Ensolite foam (same material as the rib pad typically installed outside the ribs on the dummy) was mounted to the rib impact surface with double-sided tape. The dummy was positioned at a distance from the impactor so that the piston driving the probe would no longer be accelerating prior to impacting the dummy. The center of the probe face was 30 mm above the top of the rib being impacted. Figure 7 shows the test setup for posterior and anterior impacts.

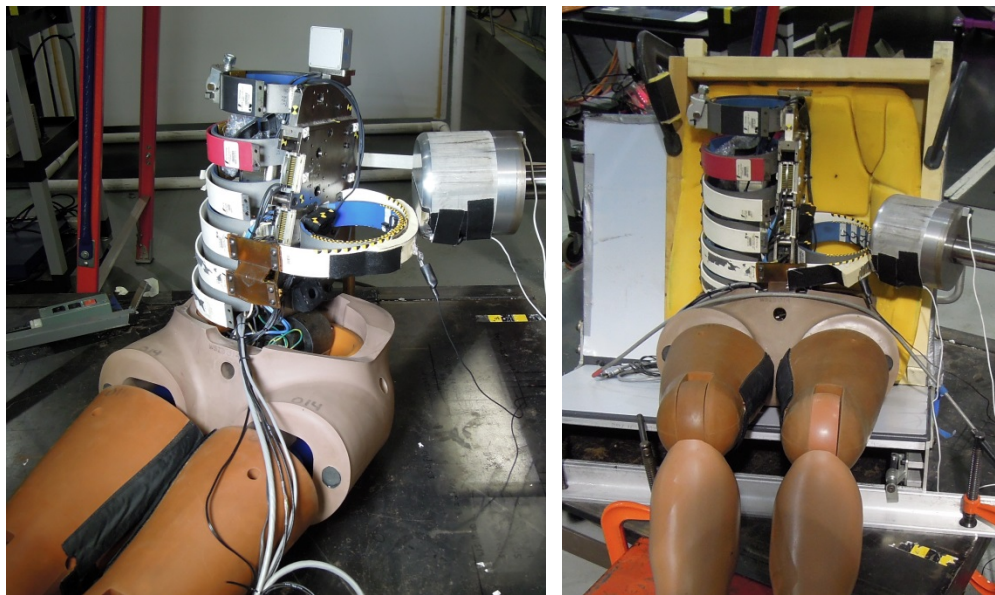


Figure 7. Test setup for 30° posterior-to-lateral (left) and 20° anterior-to-lateral (right) impacts

Fiducial targets with a 6 mm diameter were placed along the top surface of each inner rib for video tracking (33-39 targets depending on the rib) as shown in Figure 8. Targets appearing on the outer rib band were not used in this analysis. A high-speed video camera captured an

² *Evaluation of RibEye Installed in the WorldSID 50th Percentile Male Dummy*, a report still being prepared by NHTSA's Vehicle Research and Test Center

overhead view of the dynamic rib motion during impact at 1000 frames per second. The x and y position of multiple targets on the rib surface were tracked at every millisecond for the duration of the event using TEMA³ video analysis software (Image Systems AB). A target was placed in the view of the camera to indicate the location of the translated RibEye origin at the level of the rib of impact, which was used as the origin in TEMA. Figure 8 shows a view of thorax rib 3 prior to impact, denoting the origin and other points of interest.

³ TEMA has been used in many studies of motion tracking, including validation of a new kind of motion tracking system in the following papers: Reed, M., Park, B.-K. D., Ebert, S., Hallman, J., & Sherony, R. (2018, September). *Marker-less tracking of head motions in abrupt vehicle manoeuvres* IRCOBI Conference Proceedings; and Park, B.-K. D., Jones, M., Miller, C., Hallman, J., Sherony, R., & Reed, M. (2018). *In-vehicle occupant head tracking using a low-cost depth camera* (SAE Technical Paper 2018-01-1172). Warrendale, PA: SAE International. doi:10.4271/2018-01-1172.

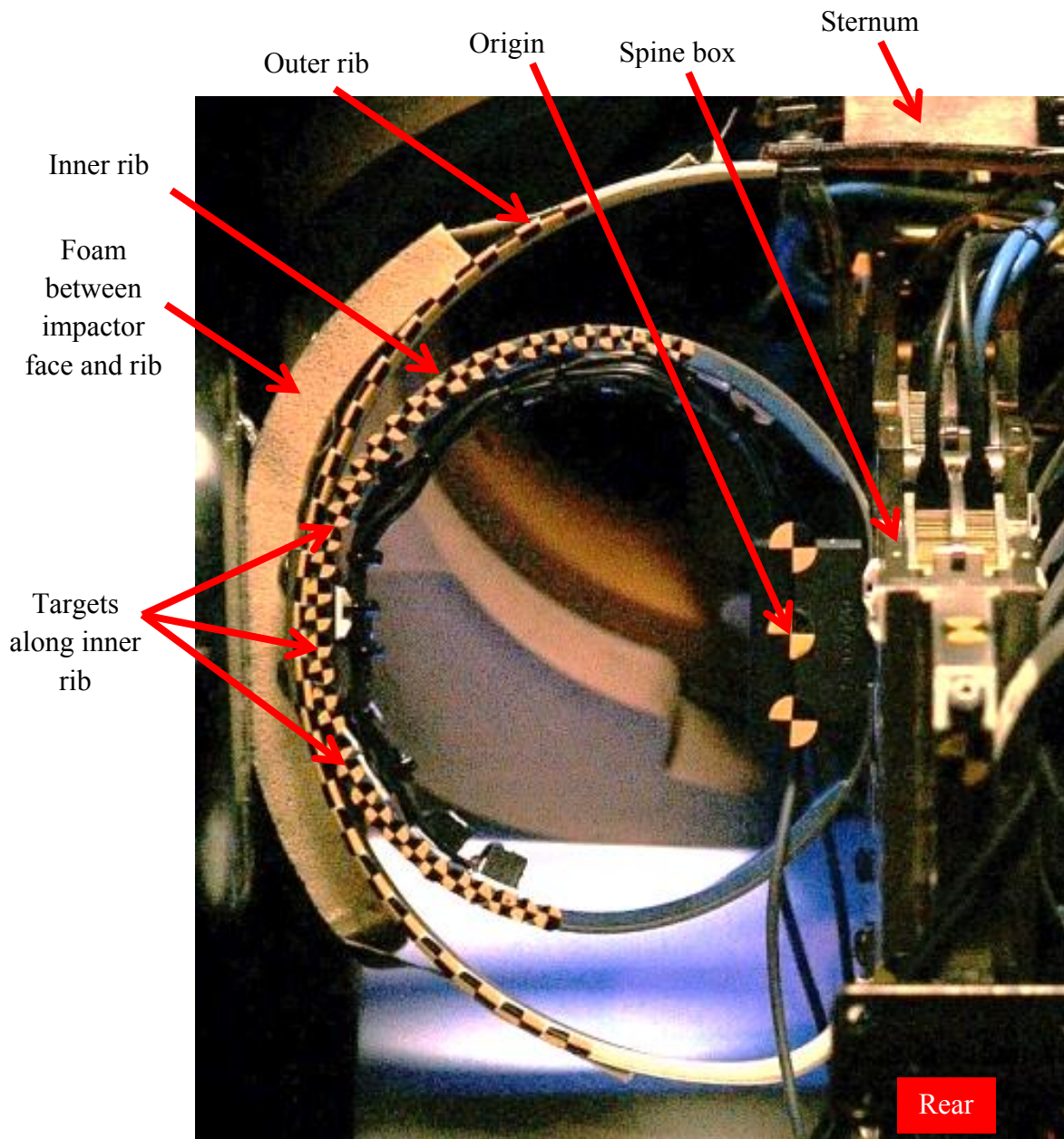


Figure 8. Pre-impact image for thorax rib 3 impacts. (Note that multiple RibEye LEDs are mounted on the inner surface of the rib. This data is discussed in the previously referenced report that evaluates the usefulness and accuracy of RibEye measurements.)

2.2 Predicted Deflection at Virtual RibEye LED Locations

The x and y position data for each fiducial target in dynamic testing was used to calculate the predicted deflection of an adjacent VR LED. In other words, it was assumed for each target that an imaginary RibEye LED was mounted on the adjacent inner surface of the rib. Each imaginary, or virtual, RibEye LED (VR) was initially positioned along a straight line in the horizontal (xy) plane between the fiducial target and the coordinate system origin (Figure 9). For thorax rib 1, the VR LEDs were assumed to be fixed to the inner surface of the rib with the sensing face at an offset distance (OD) perpendicular to the surface of the rib nominally 8 mm from the center of the target (Figure 10). For thorax ribs 2 and 3, the nominal offset distance from the sensing face of the VR LEDs to the target was 12 mm, because of the angled LED mounts on these ribs. For each target, the initial distance from the origin to the target (td_0) was calculated as shown in Equation 4 as a function of the target's tracked x and y coordinates (tx , ty). The resultant distance from the fiducial target to the VR LED (d_{VR}) was calculated as shown in Figure 10 and Equation 5. The initial distance from the origin to the VR LED location (d_0) was calculated as shown in Equation 6. It is assumed that the VR LED is rigidly attached to the rib such that the distance d_{VR} is constant for each VR LED location in each test.

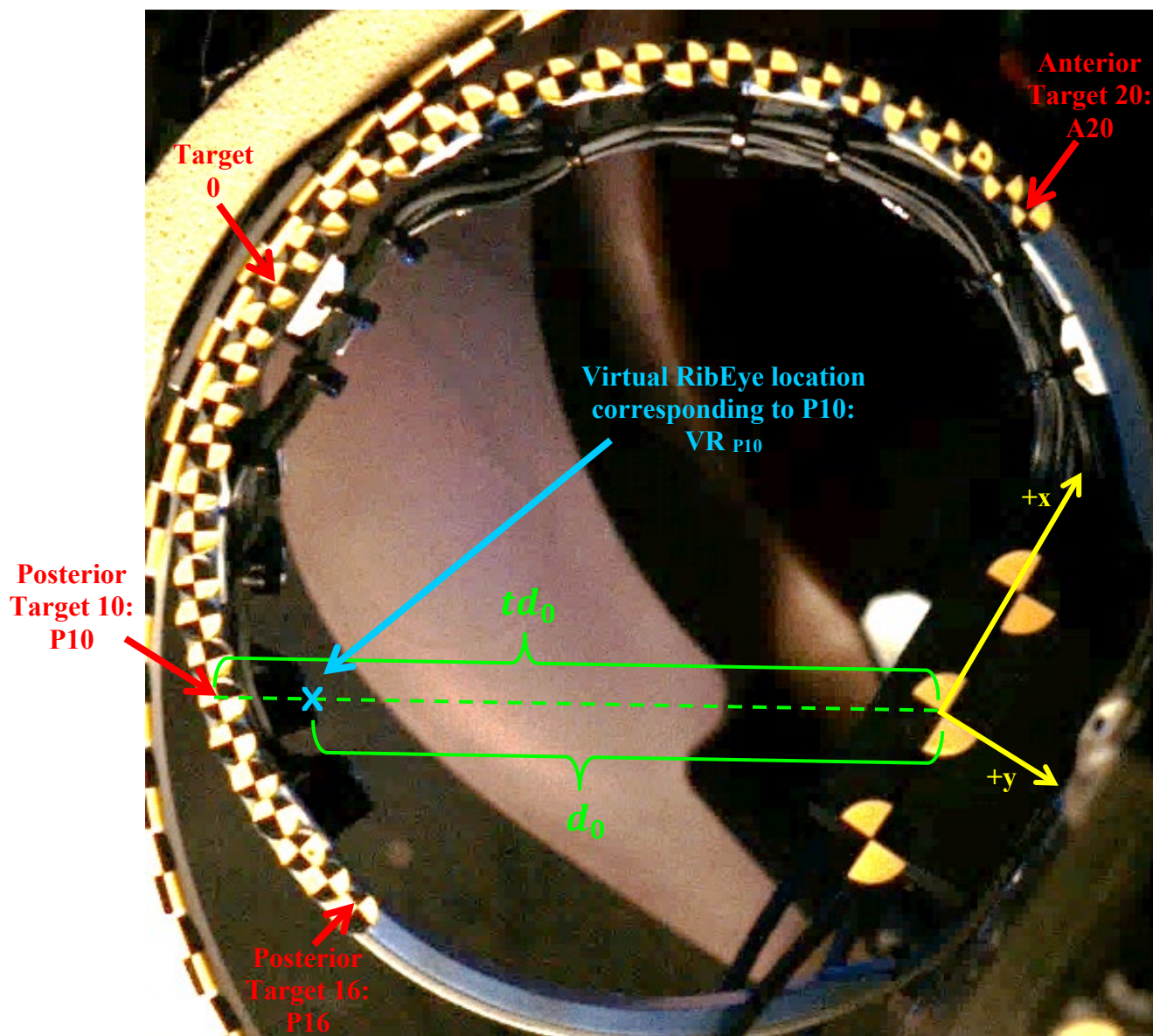


Figure 9. Initial position of Virtual RibEye LED corresponding to target P10 on thoracic rib 3

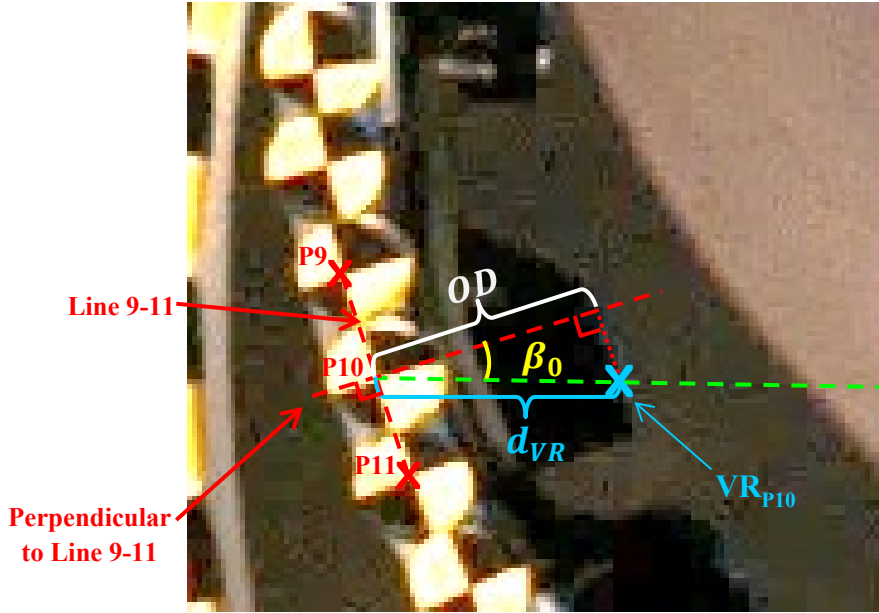


Figure 10. Close-up of initial position of Virtual RibEye LED corresponding to target P10 on thoracic rib 3

$$td(t) = \sqrt{tx(t)^2 + ty(t)^2} \quad (4)$$

$$d_{VR} = \frac{OD}{\cos\beta_0} \quad (5)$$

$$d_0 = td_0 - d_{VR} \quad (6)$$

To calculate the initial rib angle, β_0 , at the fiducial target location, first a line was drawn between the centers of the targets *anterior and posterior* to the target of interest (Line 9-11 in Figure 10). Then a perpendicular line was drawn to Line 9-11, through the center of fiducial target P10. The angle between this perpendicular line and the line connecting the target to the origin at time zero is β_0 . As the rib deforms, the VR LED location defined prior to deformation does not necessarily remain on the line between the tracked fiducial target and the origin (Figure 11). The rib angle, $\beta(t)$, can be calculated at any time point during the dynamic tests. The angle $\delta(t)$ is shown in Figure 12 and defined in Equation 7 to represent how far the VR LED location at time t has rotated away from its original location on the line between the tracked fiducial target and the origin.

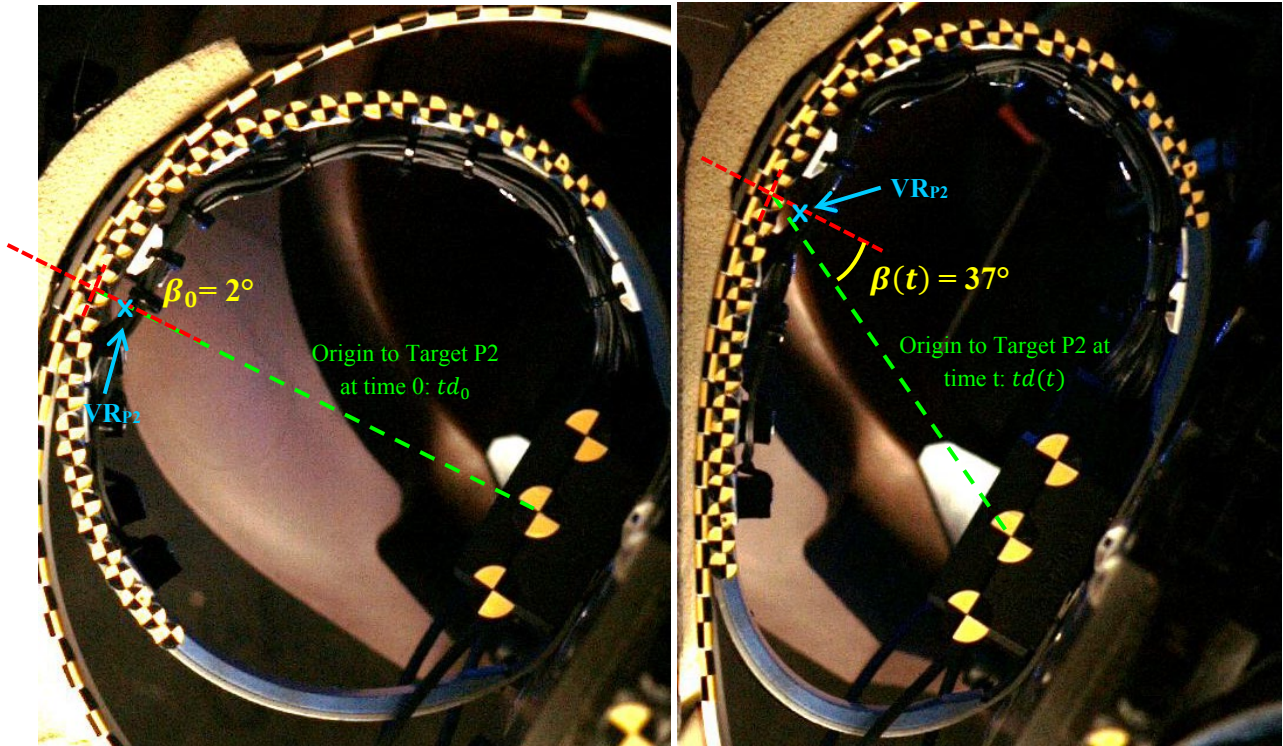


Figure 11. Rib angle $\beta(t)$ of Virtual RibEye location corresponding to target P2 on thoracic rib 3 in dynamic test 30 degrees posterior-to-lateral

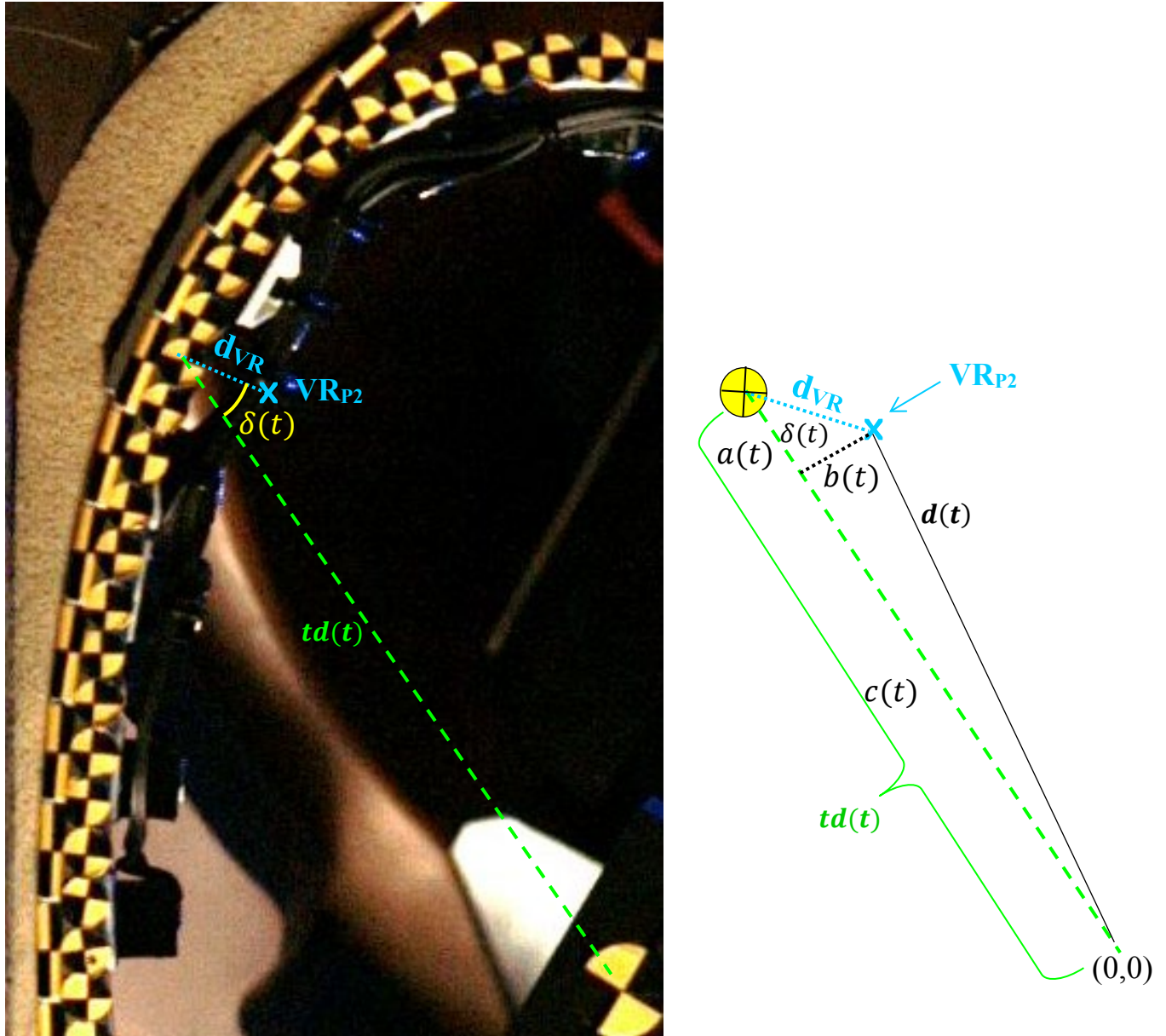


Figure 12. Calculation of distance $d(t)$ from VR LED to origin at time t

$$\delta(t) = \beta(t) - \beta_0 \quad (7)$$

At any given point in time, the distance from the VR LED to the origin, $d(t)$, can be calculated using the deformation angle $\delta(t)$ of the deformed rib and the resultant distance from the tracked fiducial target to the origin at time t , $td(t)$. These calculations are illustrated using intermediate calculations for the dimensions $a(t)$, $b(t)$, and $c(t)$ shown in Figure 12, and detailed by Equations 8-11.

$$a(t) = d_{VR} \cos \delta(t) \quad (8)$$

$$b(t) = d_{VR} \sin \delta(t) \quad (9)$$

$$c(t) = td(t) - a(t) \quad (10)$$

$$d(t) = \sqrt{b(t)^2 + c(t)^2} \quad (11)$$

The rib deflection ($D(t)$) at a VR location can then be calculated by subtracting its distance to the origin at any given time point ($d(t)$) from its original distance to the origin (d_0) (Equation 12).

$$D(t) = d_0 - d(t) \quad (12)$$

2.3 Methods for Optimization of RibEye LED Locations

To determine the ideal positions for three RibEye LEDs on each rib, rib deflection $D(t)$ was calculated at all available VR locations on all ribs, in all dynamic tests.

For each rib in each dynamic test, the time of maximum deflection was determined by identifying the time of maximum estimated deflection among all VR locations. For each rib in each dynamic test, all data beyond this time of maximum deflection was deleted so that all remaining analysis was performed only from time zero to the time of overall maximum rib deflection. The anterior-most and posterior-most VR locations were also eliminated from the analysis since adjacent targets on both sides of each VR location are required to calculate rib deflections (Figure 10).

For a given test at any time t , the true maximum rib deflection $D_{MAX}(t)$ was assumed to be the maximum value of the individual rib deflection estimates $D(t)$ made at each VR location. The difference between the $D(t)$ measured at an individual VR location and the estimated true rib deflection $D_{MAX}(t)$ was defined as the error, $E(t)$, at a given time point for a given VR location.

Since the goal for the selection of RibEye LED locations was to minimize error using three RibEye LEDs, the error that results from each possible combination of three LEDs was utilized. For a given test, the maximum deflection estimated using three RibEye LEDs was equal to the maximum deflection measured among the three LEDs at any given time point. Therefore, the error at a given time point for a combination of three VR locations, $E_{COMBO}(t)$, was equal to the error, $E(t)$, of the VR location in the trio with the smallest error at that time point (which corresponds to the location with the maximum deflection). In this way, the expected error ($E_{COMBO}(t)$) was calculated at all time points up to peak deflection for every possible combination of three VR LED locations in a given rib, for every dynamic test. Thus, equal

weight was given to data from 0° , $\pm 10^\circ$, $\pm 20^\circ$ and $\pm 30^\circ$ tests when computing the error, as it is not known how frequently each impact angle occurs to an occupant in crash tests.

Since ultimately the ideal combination of RibEye locations will make accurate measurements of deflection across a wide range of deflection magnitudes and in a variety of impact directions, the goal was to minimize the maximum error seen in any test. Therefore, selection of the most effective combination of three VR LED locations was based primarily on minimizing the error in the “worst case” test scenario. The “worst case” was identified as the maximum error for the combination (ECOMBO(t)) calculated at any time point for any rib in any of the dynamic tests. This process was completed for dynamic tests on the three thoracic ribs, based on the assumption that the same RibEye LED locations would be used for all ribs.

A secondary consideration in selecting the final combination of RibEye LED locations included the average error (ECOMBO(t)) calculated for the combination across all time points in all dynamic tests.

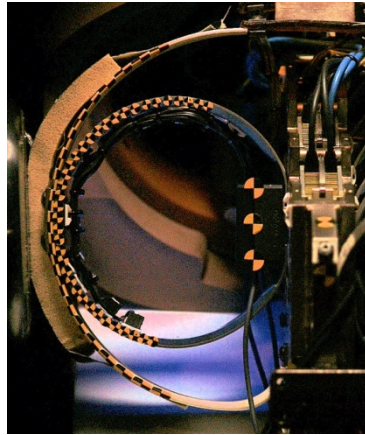
Constraints on the final selection of RibEye LED locations included the following:

1. One of the three RibEye LEDs must be located in the lateral position (same as IR-TRACC location), and
2. RibEye LEDs could practically be installed in the selected locations.

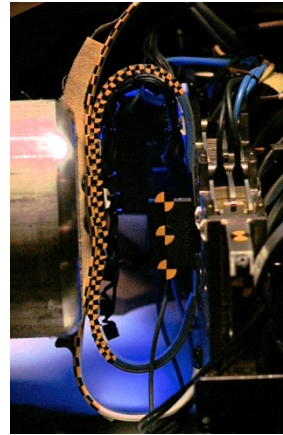
3 RESULTS

3.1 Dynamic Rib Testing

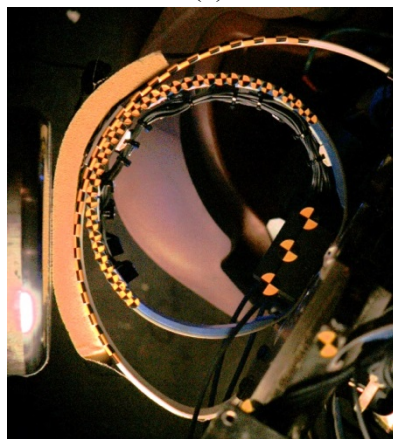
Pre-impact and maximum deflection images for thorax rib 3 pure lateral, 30° posterior, and 30° anterior impacts are shown in Figure 13.



(a)



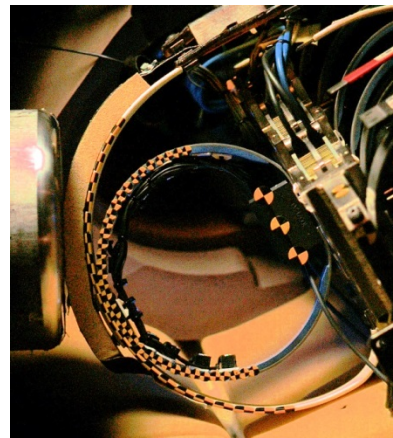
(b)



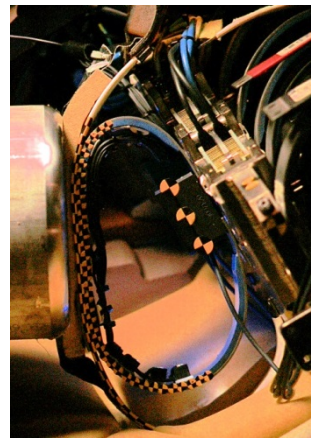
(c)



(d)



(e)



(f)

Figure 13. Pre-impact and maximum deflection images for thorax rib 3 lateral (a and b), 30° posterior (c and d), and 30° anterior (e and f) impacts. (Note that multiple RibEye LEDs are mounted on the inner surface of the rib. This data is discussed in *Evaluation of RibEye Installed in the WorldSID 50th Percentile Male Dummy*, a report still being prepared by NHTSA's Vehicle Research and Test Center.)

3.2 Combinations of RibEye LED Locations

Combinations of virtual LED locations that included an LED at the lateral position corresponding to the IR-TRACC location on the rib (constraint #1) were ranked from least to most maximum (“worst-case”) error for the combination, and secondarily from least to most mean error for the combination across all time points in all dynamic tests in all three ribs tested. The best 45 combinations are shown in Table 2. The VR locations are numbered according to the associated target used to predict the motion at each virtual location. The “0” target is the one closest to the location where an IR-TRACC would measure deflection.

For all combinations in Table 2, the worst error was associated with a test on Thoracic Rib 3. The test which produced the worst error for each combination varied: for some combinations the “worst-case” error was measured in a lateral (0 degree) test, while other combinations had “worst-case” errors in tests up to 30 degrees anterior- or 30 degrees posterior-to-lateral. Among the 45 best combinations identified, none had error of 10 mm or greater at any time point in any of the dynamic tests in any rib. For all combinations in Table 2, the mean error across all time points for dynamic tests in all ribs was less than 2.5 mm.

For the best five combinations identified (combinations A3-A7, 0, and P5 in Table 2), maximum error never exceeded 7.2 mm and averaged less than 1.5 mm. However, these combinations included RibEye locations as close as 3 to 5 target positions from the central “0” RibEye location. At these locations, the LEDs would be positioned close to or on the section of rib damping material where it is tapered (Figure 14). Although these locations would be feasible, they would not be the most practical since the angle and length of the taper in this section of material are not specified on the drawings.⁴ Thus, the position of an LED may be on the taper for one rib and not on the taper for another rib. To avoid this issue, the final locations for the LEDs were selected to be beyond the section of damping material taper, which, for the ribs that were inspected, happened to be 35 mm linearly from the center position as shown in Figure 15. The linear measurement was made from the center LED position to the edge of the mount or LED surface.

It was determined that the closest that the anterior and posterior RibEye LEDs could be mounted, relative to the central RibEye LED at the location where an IR-TRACC would be, was 6 or 7 positions from the 0 position (Figure 14). The best combination meeting this additional constraint included virtual LEDs at the central location, as well as virtual LEDs at 6 or 7 target positions anterior and 6 or 7 target positions rearward of that location. Using

⁴ WorldSID-50M Drawing Package to be published in 2019

Table 2. Maximum and mean error for the top 45 combinations of three virtual RibEye LED locations (sorted by maximum error, from least to most)

Combination			Maximum Error	Mean Error
Virtual RibEye LED locations			Maximum E _{COMBO} (t) <i>for all time points in all dynamic tests in all ribs (mm)</i>	Mean E _{COMBO} (t) <i>for all time points in all dynamic tests in all ribs (mm)</i>
A4	0	P5	7.16	0.85
A5	0	P5	7.16	0.92
A3	0	P5	7.16	0.92
A6	0	P5	7.16	1.08
A7	0	P5	7.16	1.32
A4	0	P6	9.04	0.88
A5	0	P6	9.04	0.95
A3	0	P6	9.04	0.95
A4	0	P7	9.04	0.96
A5	0	P7	9.04	1.03
A3	0	P7	9.04	1.03
A4	0	P8	9.04	1.09
A6	0	P6	9.04	1.11
A5	0	P8	9.04	1.16
A3	0	P8	9.04	1.16
A6	0	P7	9.04	1.18
A6	0	P8	9.04	1.32
A7	0	P6	9.04	1.34
A7	0	P7	9.04	1.42
A7	0	P8	9.04	1.56
A8	0	P5	9.20	1.53
A8	0	P6	9.20	1.56
A8	0	P7	9.20	1.64
A9	0	P5	9.20	1.65
A9	0	P6	9.20	1.68
A9	0	P7	9.20	1.75
A8	0	P8	9.20	1.77
A10	0	P5	9.20	1.80
A10	0	P6	9.20	1.83
A9	0	P8	9.20	1.89
A10	0	P7	9.20	1.90
A11	0	P5	9.20	1.98
A11	0	P6	9.20	2.01
A10	0	P8	9.20	2.04
A11	0	P7	9.20	2.09
A11	0	P8	9.20	2.22
A4	0	P9	9.63	1.28
A5	0	P9	9.63	1.35
A3	0	P9	9.63	1.35
A6	0	P9	9.63	1.50
A7	0	P9	9.63	1.74
A8	0	P9	9.63	1.96
A9	0	P9	9.63	2.07
A10	0	P9	9.63	2.22
A11	0	P9	9.63	2.41

Highlighted rows indicate maximum and mean E_{COMBO}(t) for final LED locations; final LED locations were between targets 6 and 7 in the anterior and posterior directions

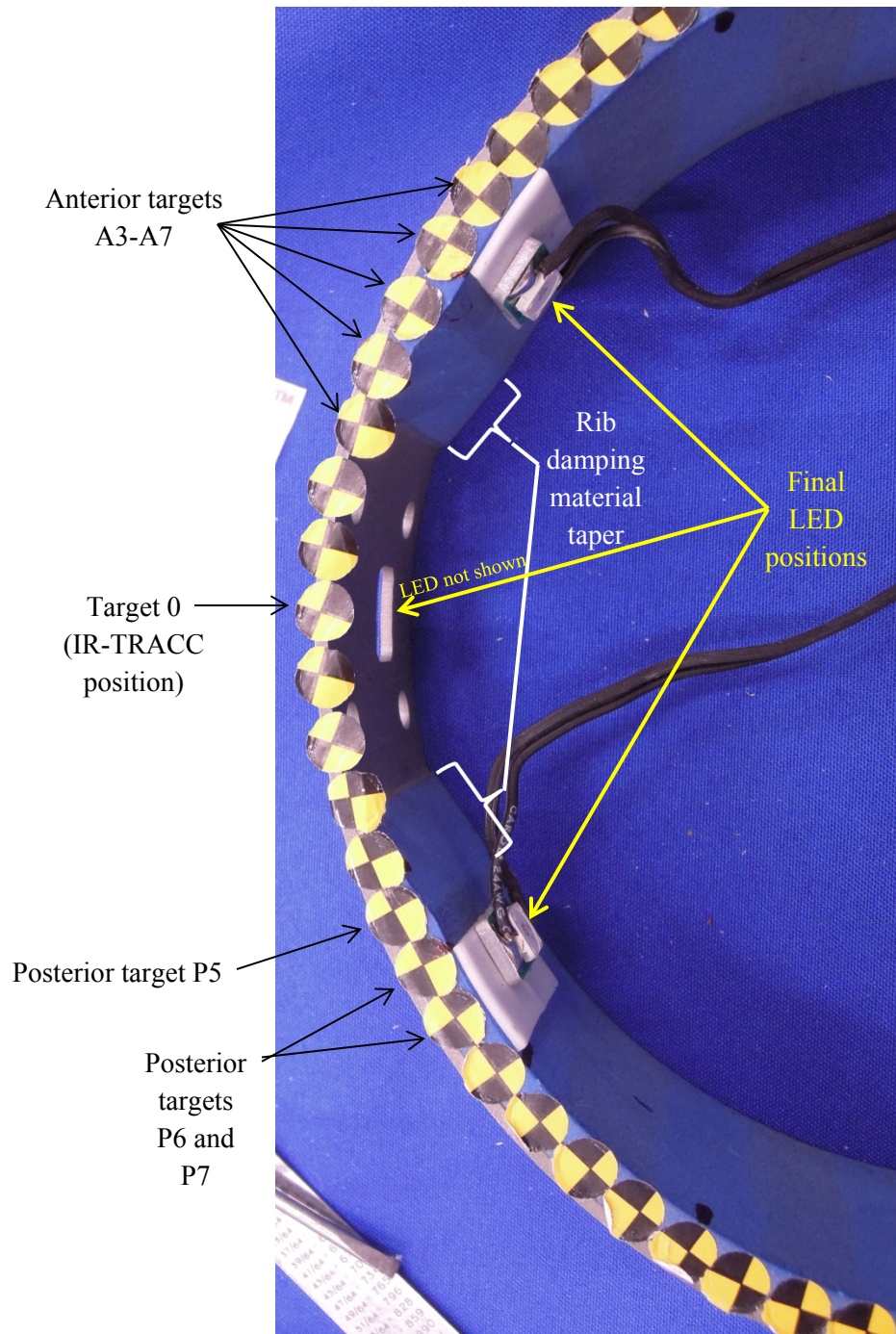


Figure 14. Image of thorax rib 1 showing final locations selected for the three LEDs, anterior and posterior targets of the five best combinations, and rib damping material taper

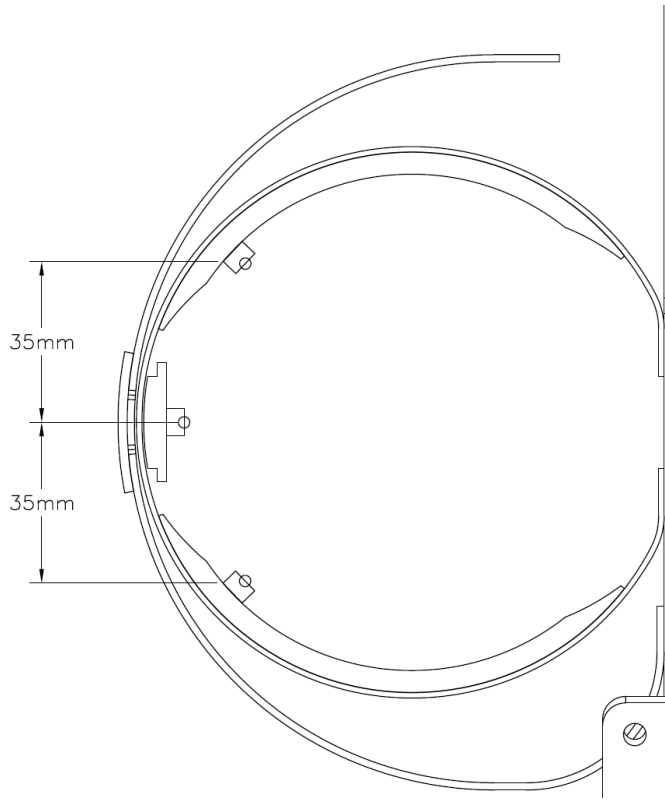


Figure 15. Schematic of a rib showing the final locations for the three LEDs

VR LEDs at these locations resulted in a worst-case error in displacement measurement of 9 mm and a mean error of 1.1-1.4 mm across all time points in all dynamic tests (see highlighted rows in Table 2).

In comparison, measuring deflection in the current tests at only a single location corresponding to the location where IR-TRACC measurements would be taken, would have resulted in a maximum error of 23 mm in the dynamic tests, and an average error of 4.7 mm across all time points in the dynamic tests.

3.3 Deflection Comparisons Among Overall Max, Max of Trio of Virtual LED Positions, and IR-TRACC

Figure 16 shows deflection time histories for +20° and +30° dynamic impact tests for thorax ribs 1-3 for three virtual LED scenarios: 1) overall max deflection (DMAX), 2) the max deflection from a combination of three virtual LED positions with the least amount of error after considering practical installation limitations (P6/0/A6), and 3) the IR-TRACC location.

Similarly, Figure 17 and Figure 18 show deflection time histories for dynamic impact tests at -30°, -20°, -10°, 0°, and +10°. Figure 19 shows maximum deflection for each virtual LED position for each dynamic impact test for thorax ribs 1-3, along with the final LED locations identified. For example, the center red line indicates the location of the middle LED and the IRTRACC, the left red line indicates the location of the front LED, and the right red line indicates the location of the rear LED. The measurements at these locations (intersection of the red lines and each curve) can be compared to the maximum deflection measured in each impact test (maximum of each curve).

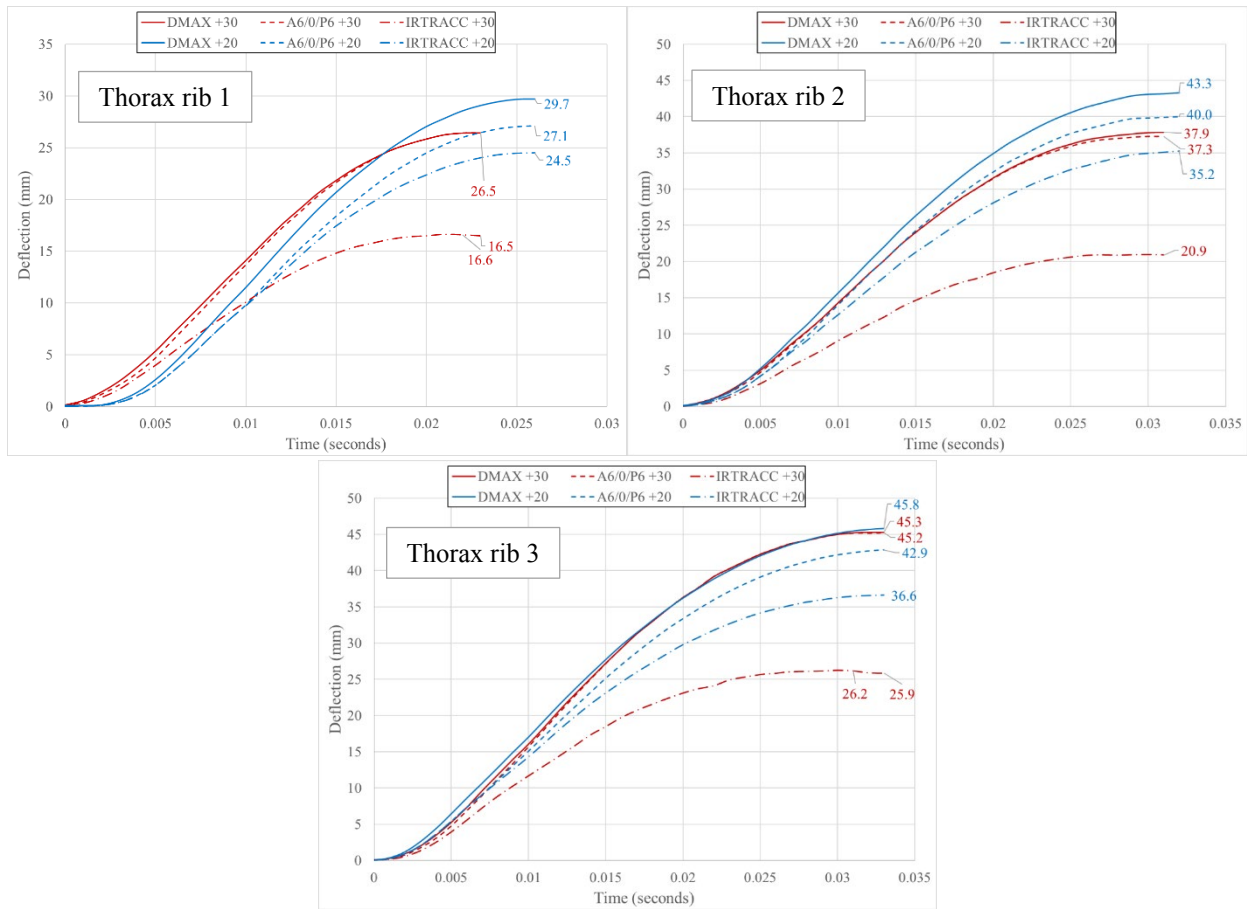


Figure 16. Deflection time histories for overall max deflection, A6/0/P6 combination, and IRTRACC location for +30° and +20° dynamic impact tests for thorax ribs 1, 2, and 3

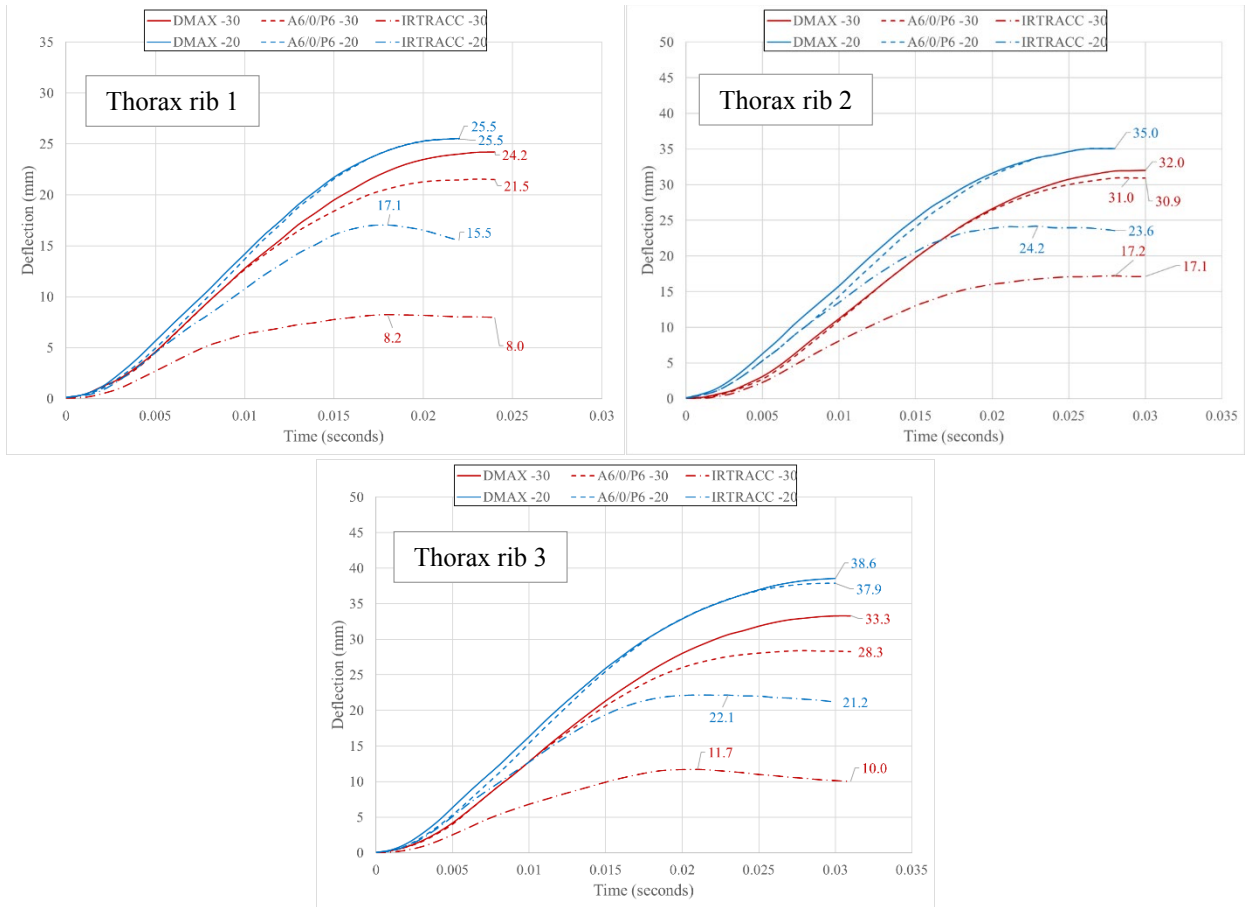


Figure 17. Deflection time histories for overall max deflection, A6/0/P6 combination, and IR-TRACC location for -30° and -20° dynamic impact tests for thorax ribs 1, 2, and 3

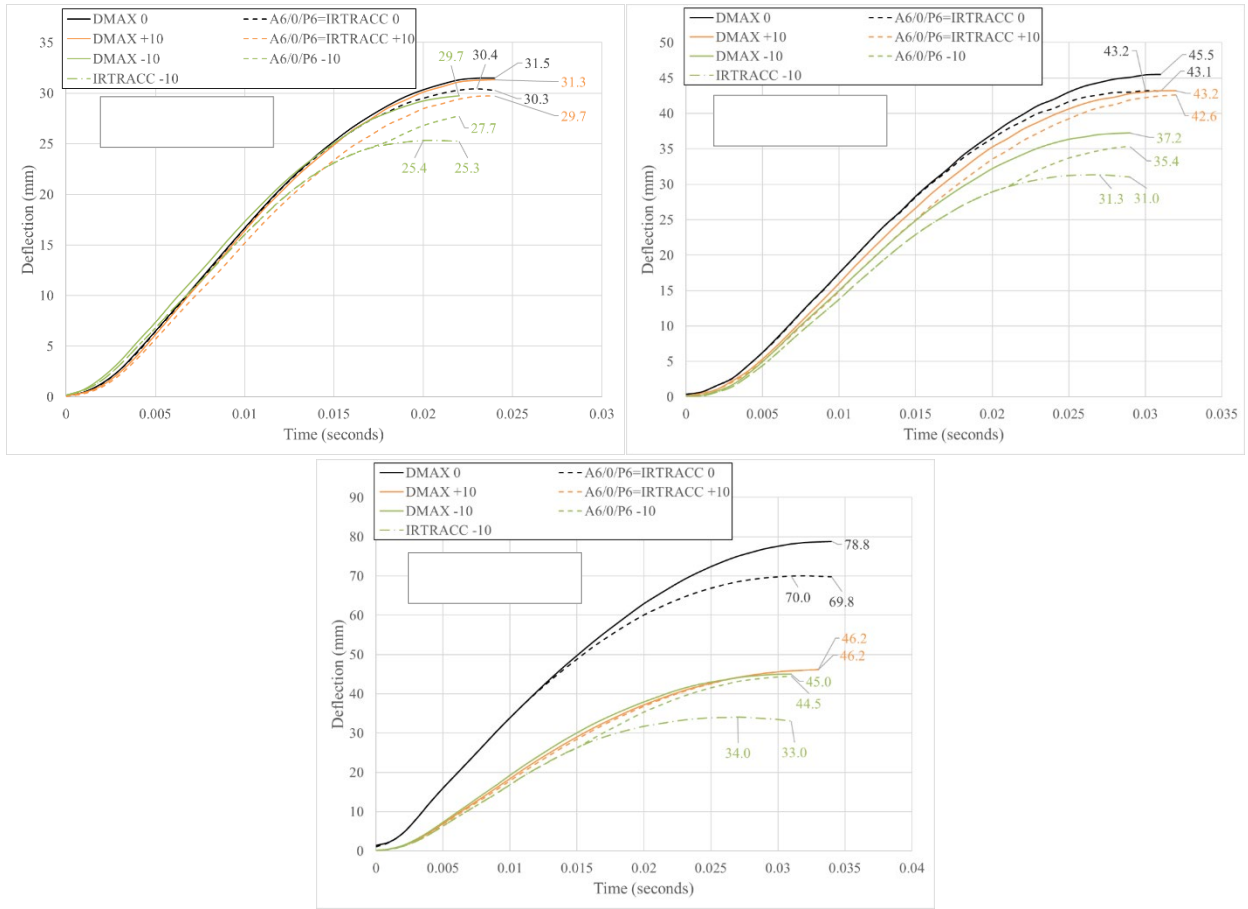
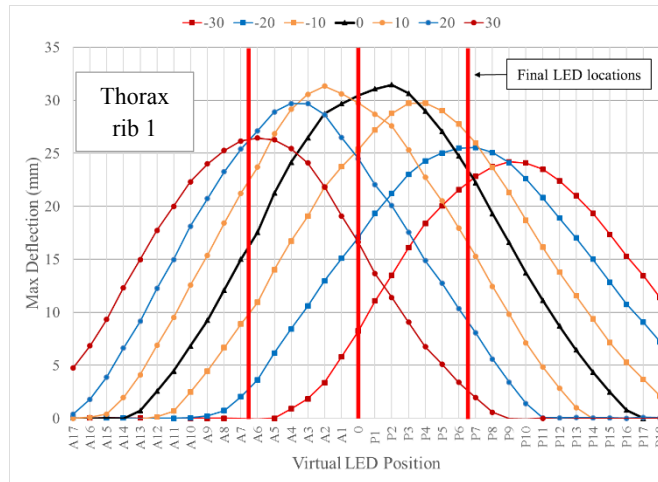
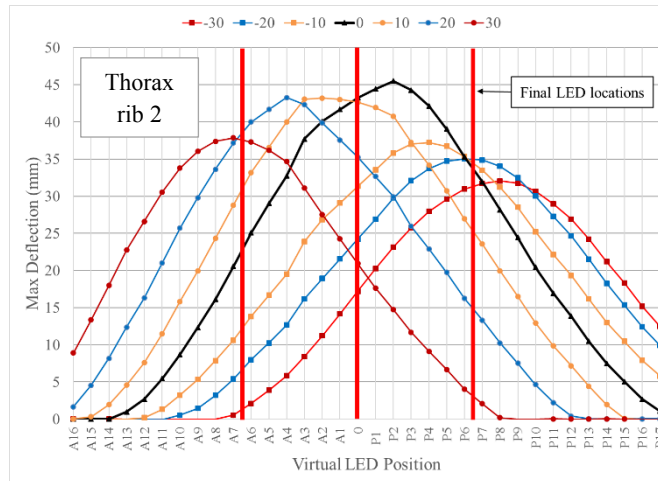


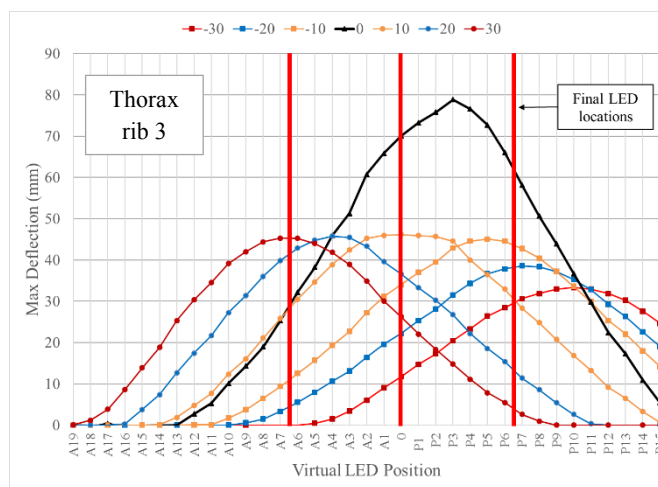
Figure 18. Deflection time histories for overall max deflection, A6/0/P6 combination, and IRTRACC location for +10°, -10°, and 0° dynamic impact tests for thorax ribs 1, 2, and 3



(a)



(b)



(c)

Figure 19. Max deflection for each virtual LED position for thorax rib 1 (a), thorax rib 2 (b), and thorax rib 3 (c) in all dynamic rib impacts

4 DISCUSSION

4.1 Deflection Comparisons Among Overall Max, Max of Trio of Virtual LED Positions, and IR-TRACC

Figures 16-18 compare time histories for the various impact conditions for three virtual LED scenarios: 1) overall max deflection (D_{MAX}), 2) the max deflection from a combination of three virtual LED positions with the least amount of error after considering practical installation limitations (P6/0/A6), and 3) the IR-TRACC location. Figure 16 shows that for thorax ribs 1-3 in the +30° condition the overall max deflection and the A6/0/P6 trio max were almost identical, and the IR-TRACC location was between 10-19 mm less at the peak deflection. For thorax ribs 1-3 in the +20° condition the IR-TRACC location was between 5-9 mm less than the overall maximum at the peak, and the A6/0/P6 trio max was within 3 mm of the overall max at the peak. Figure 17 shows that for thorax ribs 1-3 in the -30° condition, the A6/0/P6 trio max is within 5 mm of the overall max at the peak, whereas the IR-TRACC location is between 15-22 mm less than the overall max. It is also noteworthy that the max deflection at the IR-TRACC location occurs earlier in time than the max deflection at either the overall max deflection location or the A6/0/P6 max location, which is true for both the -30° and -20° conditions. For the -20° condition, the overall max and A6/0/P6 max were almost identical, but the IR-TRACC was between 8-17 mm less than the overall max. Figure 18 shows that for thorax ribs 1-3 in the 0° condition, the A6/0/P6 max and IR-TRACC locations are the same, giving the same deflections. This is also true in the +10° condition. For thorax ribs 1-2 in the 0° and +10° conditions, the A6/0/P6 max and IR-TRACC are within 2 mm from the overall max. However, for thorax rib 3 in the 0° condition, the A6/0/P6 max and IR-TRACC are within 9 mm of the overall max at the peak. For thorax rib 3 in the +10° condition, the A6/0/P6 max and IR-TRACC are almost identical to the overall max. For thorax ribs 1-3 in the -10° condition, the A6/0/P6 max is within 2 mm and the IR-TRACC is between 4-6 mm less than the overall max deflection. Although it would be expected that the lateral-most location (IR-TRACC or “0” location) would measure the max deflection in a lateral test, the WorldSID-50M ribs deform such that the ribs roll slightly toward the front of the dummy in a lateral load condition (see Figure 13b). Figure 19 shows that for thorax ribs 1 and 2 in the 0° test, the max deflection occurs at virtual LED position P2 and the lateral-most location (virtual LED position “0”) deflects a couple millimeters less. However, for thorax rib 3 in the 0° test, the max deflection occurs at virtual LED position P3 and the lateral-most location (virtual LED position “0”) deflects almost 9 mm less. This is a result of the way the WorldSID-50M ribs deflect. Using thorax rib 1 results as an example, if only a single measurement was located at the middle LED/IRTRACC position, it would underestimate the maximum deflection in every impact direction, only by a few millimeters for the 0°, +10° and -10° impacts, but up to 16 mm for the -30° impact direction. However, if three measurements are

taken at the locations of the three red lines (front, middle, and rear LED locations), the maximum deflection was only underestimated at the most by 2.6 mm.

To summarize the difference between the overall max deflection (DMAX) and the maximum deflection that would have been reported from the A6/0/P6 and IR-TRACC locations, Figure 20 shows that for the 0° and +10° conditions the IR-TRACC and A6/0/P6 reported the same max deflections (and the same difference from the overall max deflection). As the impact direction becomes more oblique, the difference in max deflection between the overall max and that reported from the IR-TRACC increases. The A6/0/P6 trio reports differences from the overall max that are much less on average as compared to the IR-TRACC, with the greatest difference being 9 mm. It is clear that measuring deflection in multiple (optimal) locations on a rib will result in better estimates of the true maximum deflection as compared to measuring at a single location. Although the impact conditions utilized here may not be representative of all conditions that a dummy may encounter, they do represent a range of impact directions that may occur due to various occupant loadings that occur in a vehicle crash.

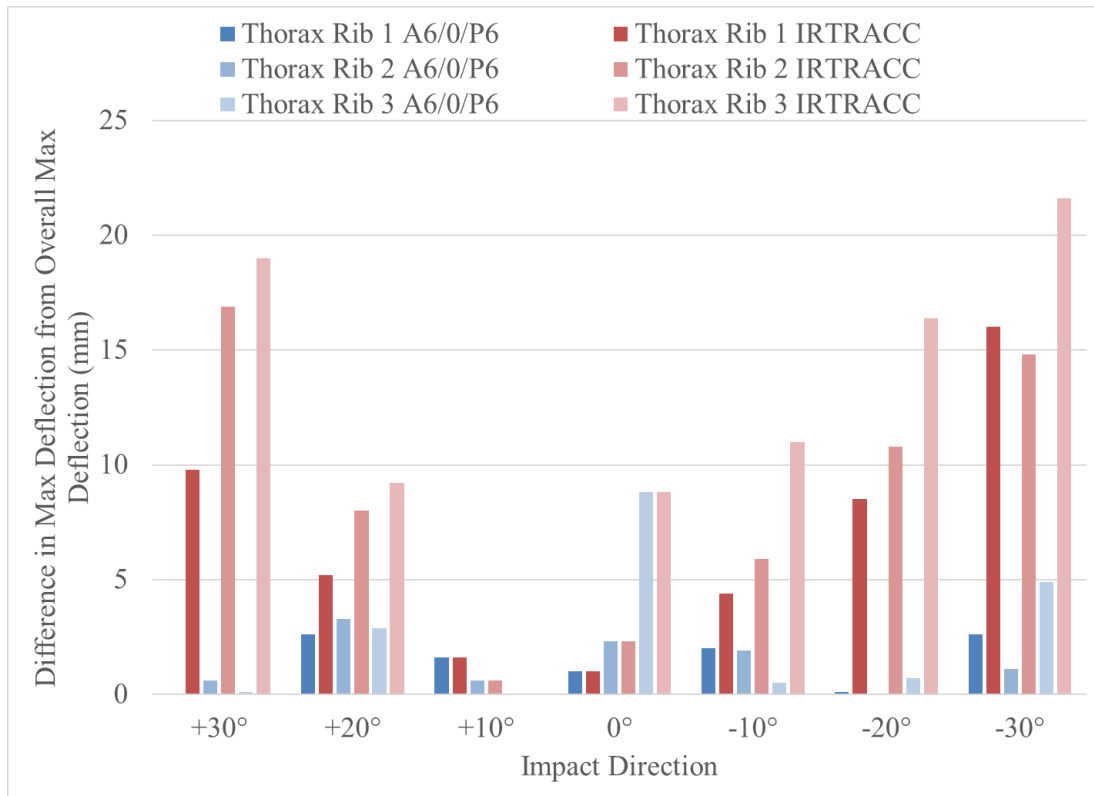


Figure 20. Differences in max deflection reported between overall max deflection and A6/0/P6 and IR-TRACC locations

5 CONCLUSIONS

Dynamic impact tests were performed on single ribs of the WorldSID-50M dummy at multiple angles anterior-to- and posterior-to-lateral, as well as pure lateral. High-speed video was used to track the position of multiple targets located on the top surface of the rib. This position data was used to locate VR LEDs corresponding to each target throughout each test. Deflection measurements for each virtual LED location were calculated, from which the combination of three LED locations with the least maximum error was identified. As the virtual LED locations with the least maximum error occurred in areas where the taper of the damping material exists, the final LED locations were adjusted so as not to be positioned within the section of taper. The maximum error calculated from the dynamic rib tests for the final combination of three LED positions is 9 mm, which is less than the maximum error of 23 mm calculated from the dynamic rib tests for the location of the IR-TRACC in the current dummy design. These final LED positions will be used in further testing (sled and crash) to evaluate the feasibility of the RibEye in the WorldSID-50M.

DOT HS 812 758
July 2019



U.S. Department
of Transportation
**National Highway
Traffic Safety
Administration**

